Sensors & Actuators: B. Chemical 284 (2019) 444–450

Contents lists available at ScienceDirect

Sensors and Actuators B: Chemical

journal homepage: www.elsevier.com/locate/snb

Real-time selective detection of 2-chloroethyl ethyl sulfide (2-CEES) using an Al-doped ZnO quantum dot sensor coupled with a packed column for gas chromatography

Jun Ho Lee[a], Hwaebong Jung[a], Ran Yoo[a], Yunji Park[a], Hyun-sook Lee[a], Yong-Sahm Choe[b], Wooyoung Lee[a,*]

[a] Department of Materials Science and Engineering, Yonsei University, 50 Yonsei-ro, Seodaemun-gu, Seoul 03722, Republic of Korea
[b] iSenlab Inc., Halla Sigma Valley, Dunchon-daero 545, Jungwon-gu, Seongnam-si, Gyeonggi-do, 13215, Republic of Korea

ARTICLE INFO

Keywords:
Gas sensor
Miniaturized gas chromatography
Al-doped ZnO quantum dots
2-CEES
Mustard simulant
Packed column

ABSTRACT

We report a new portable chemical warfare agent analyzer for miniaturized gas chromatography (mini-GC), comprising a packed column and hydrothermally synthesized Al-doped ZnO quantum dots (AZO QDs). This device uses a small volume of the target gas (1 ml) without pre-concentration and can be used to detect 2-chloroethyl ethyl sulfide (2-CEES) gas, which is a mustard gas simulant, over a wide concentration range. The AZO QD (~5 nm) sensor exhibited an outstanding sensing response (R) of 5,393 in detecting 20 ppm of 2-CEES; this performance is superior to those of other previously reported 2-CEES sensors based on semiconducting metal oxides. By optimizing the length of the packed column, we successfully decreased the retention time of 2-CEES to ~150 s. More importantly, the manufactured mini-GC device can be used to selectively detect a small amount of target gas from other gases such as NH_3, NO, and CO. We demonstrated the excellent detection performance of the device for the real-time selective detection of 2-CEES.

1. Introduction

Chemical warfare agents (CWAs) have been developed and utilized for military purposes owing to their relatively easy manufacturing process and extremely toxic properties, which can lead to incapacitation and can be fatal [1–3]. Such gases are classified into five main categories based on their effects: blister, nerve, choking, asphyxiants, and behavior altering agents. In particular, blister agents or vesicants are a class of chemicals capable of causing severe blisters on human skin. Mustard gas, which is an example of a blister gas, is infamous for its highly fatal use in battlefields since World War I and is responsible for approximately 70% of the casualties who suffered from toxic gases during the war. It may even affect the division of cells by irreversibly alkylating the DNA, RNA, and proteins [1]. The fear of being exposed to such gases and the threats of terrorism have led to the development of techniques to detect CWAs; such techniques include ion mobility spectrometry (IMS) [4], gas chromatography-mass spectrometry (GC–MS) [5], proton-transfer-reaction mass spectrometry (PTR-MS) [6], and Raman spectroscopy [7,8]. However, these techniques are complex, expensive, immobile, and time-consuming, making them inappropriate for applications in warfare. To overcome these obstacles, metal oxide-based semiconductors have been studied as chemoresistive sensors; some of them are capable of detecting low concentrations of CWA simulants such as DMMP [9–11] and CEES [12–14]. Despite their excellent sensing performances, their selectivity remains unclear [15].

Previously, our group reported that Al-doped ZnO nanoparticles (AZO NPs, d = ~30 nm) have a significantly high sensing performance toward one of the mustard simulants among CWAs, i.e., 2-chloroethyl ethyl sulfide (2-CEES) [16,17]. To our knowledge, the response of AZO NPs (R = 954.2) to 20 ppm of 2-CEES at 500 °C is the best sensing performance so far [17]. However, it is well known that most metal oxide-based semiconducting sensors are limited by the lack of selectivity of the target gas to other gases, and the same is true for sensors based on AZO NPs. To overcome the selectivity problem associated with AZO NPs, we previously developed a device comprising a miniaturized GC column integrated with ZnO quantum dots (ZO QDs, d = ~5 nm) for detecting acetone from human breath [18]. The mini-GC device can be used to detect acetone from small amounts of human breath (1 ml) with high sensitivity and selectivity.

Here, we investigate the sensing performances of AZO NPs and QDs incorporated in a mini-GC device for the selective detection of 2-CEES. We discuss the size effect of the AZO particles on the sensing

* Corresponding author.
E-mail address: wooyoung@yonsei.ac.kr (W. Lee).

https://doi.org/10.1016/j.snb.2018.12.144
Received 13 August 2018; Received in revised form 12 December 2018; Accepted 27 December 2018
Available online 27 December 2018
0925-4005/

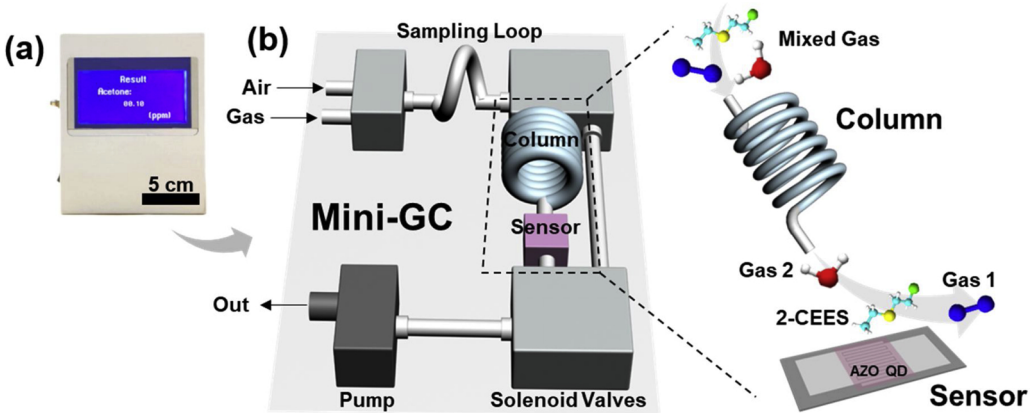

Fig. 1. (a) Real image of the mini-GC device, and (b) a schematic of its interior components.

performance in the detection of 2-CEES. We then study the selectivity of the mini-GC device integrated with AZO QDs by mixing the target gas with interfering gases such as NH_3, NO, and CO in an ambient condition. The mini-GC device integrated with the AZO QDs was found to be capable of selectively detecting 2-CEES.

2. Materials and methods

2.1. Synthesis and characterization of sensing materials

Undoped ZO QDs and AZO QDs were fabricated using a wet chemical method. For synthesizing ZO QDs, Zn acetate ($Zn(O_2CCH_3)_2$, Alfa Aesar) was used as a Zn precursor. The ZnO precursor solution was prepared by dissolving 1.975 g of Zn acetate in 90 ml of *N,N*-dimethylformamide ($(CH_3)_2NC(O)H$, Duksan). The solution was then slowly injected using a syringe pump into a methanolic solution of tetramethylammonium hydroxide (TMAH, $N(CH_3)^{4+}(OH)^-$ (methanol-tetramethylammonium hydroxide = 1:8)) at a rate of 7 ml/min and stirred for an hour at 30 °C. After stirring, the synthesized QDs were centrifuged and cleansed using acetone. The final products were dispersed in methanol. For synthesizing AZO QDs, 1 at% of Al precursor ($Al(O_2CCH_3)_3$, Alfa Aesar) was added to the Zn precursor solution. This specific doping concentration was selected, because it showed the best sensing property among Al-doped ZnO nanoparticles [14]. The fabricated ZO and AZO QDs were approximately 5 nm in size. The phase structure and morphology of the as-synthesized particles were characterized using an X-ray diffractometer (XRD, Ultima IV/ME 200DX, Rigaku) with Cu Kα radiation and a field-emission transmission electron microscope (FE-TEM, JEOL JEM ARM 200 F), respectively. A more detailed explanation on the synthesis and characterization of QDs is given in our separate report [19]. To compare the sensing properties of undoped ZnO and AZO QDs with those of NPs, the ZO NPs and AZO NPs were synthesized using a hydrothermal method. The experimental details of the procedure can be found in our previous works [17,18].

2.2. 2-CEES gas sensing in a tube furnace system

First, to fabricate sensors for a tube furnace system, an interdigitated Pt electrode was patterned on a SiO_2 substrate. To provide good contact between the Pt layer and the SiO_2 substrate, a Cr layer was used as an interlayer. The Cr (20 nm) and Pt (100 nm) layers were deposited on the SiO_2 substrate using a DC sputtering system. Subsequently, the ZnO-based NPs and QDs were loaded on the interdigitated Pt electrode using different methods. For the undoped ZnO and AZO NPs, the synthesized powders were mixed with α-terpinol paste, and the mixture was spread on the Pt electrode. To remove the binding agent and enhance the stability of the sensor, the samples were dried at 300 °C for 1 h and annealed at 600 °C for another hour. For the undoped ZnO and AZO QDs, the QD solutions were dispersed by ultrasonication and spread on the interdigitated Pt electrode using a dropping method. To remove the solvent and enhance the stability of the sensor, the samples were heat treated at 600 °C for 30 min.

After sensor fabrication, the sensor devices were mounted on a chamber in a tube furnace equipped with mass flow controllers (MFCs) for gas sensing tests. The gas mixture containing 2-CEES and air was produced by varying the gas flow rates using the MFCs, and the gas flow was kept constant at 1000 sccm. The sensing properties of the sensors were measured at 450 °C using a combination of a current source (Keithley 6220) and a nanovoltmeter (Keithley 2182). The sensor response measured in a tube furnace system can be defined as follows:

$$\textit{Sensor Response}\ (R) = \frac{R_a - R_g}{R_g} \quad (1)$$

where R_a and R_g are the sensor resistances under air and target gas, respectively.

2.3. 2-CEES gas sensing in a miniaturized gas chromatography (mini-GC) device

The mini-GC device comprises a loop for sampling the target gas, a packed GC column, three solenoid valves, a mini pump, and a sensor based on ZnO particles [18]. Fig. 1(a) and (b) show an image of the instrument and a schematic of the interior components of the mini-GC device, respectively. The actual dimensions of the mini-GC device are $8 \times 13 \times 16\ cm^3$. The nanoparticles for the device were prepared using an Al_2O_3 substrate with interdigitated Pt electrodes. The undoped ZnO and AZO NPs sensors were fabricated by mixing nanoparticle powders with α–terpinol paste and loading the mixture onto to the Pt electrodes. After loading, the sensors were heated to 300 °C for 30 min and 600 °C for 30 min with a heat rate of 5 °C/min. On the other hand, the undoped ZnO and AZO QDs sensors were fabricated by dropping each solution on the Pt electrodes and heating at 600 ℃ for 30 min.

The sensing process of the manufactured mini-GC device is as follows: First, 1 ml of ambient air and target gas were injected into the device using a mini-pump. The mixed gas was collected in the sampling loop without pre-concentration. Subsequently, the injected gas mixture moved further into the packed column and was separated to each component of gas with the help of the carrier gas (air) while passing through the column. The target gas was detected using the undoped ZnO and AZO gas sensors attached at the end of the column after a few minutes from injection. The inner diameter of the column was 0.15 cm. The column is filled with a supporter, CarboBlack B, coated with a stationary phase, CarboWax 20 M. The length of the column was varied from 20 cm to 5 cm in order to change the retention time of the target gas. Each end of the fillers was blocked by a pile of glass wool. The operation temperature of the column was set to maintain 30 ℃.

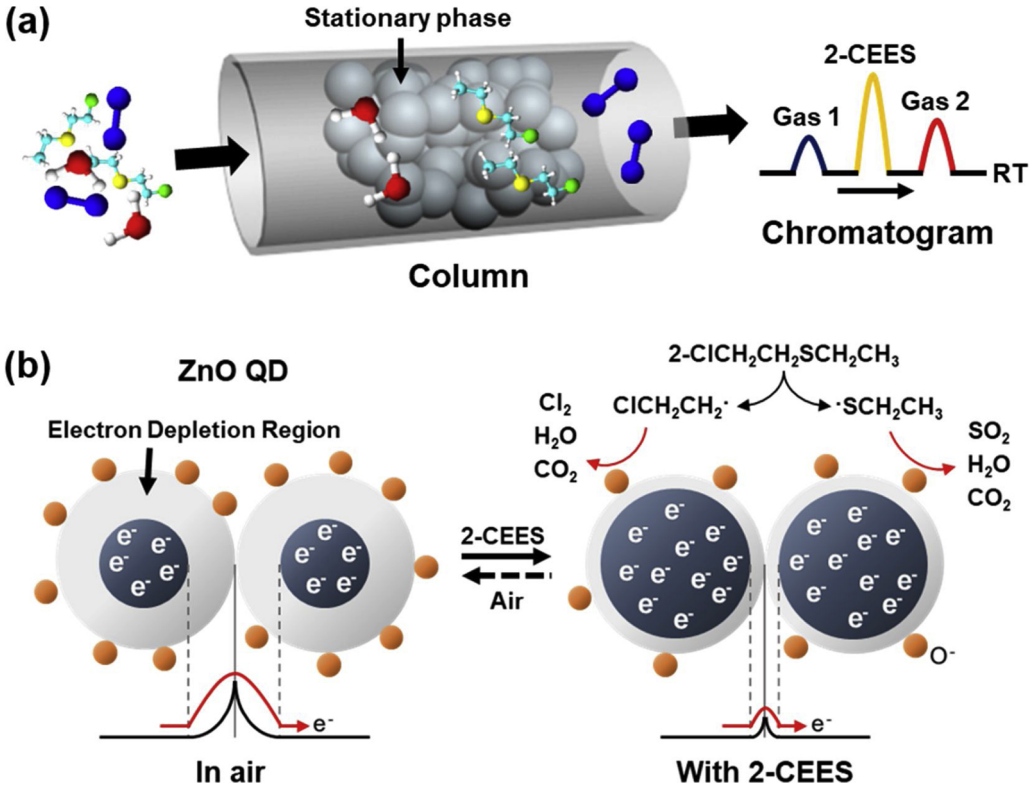

Fig. 2. Schematic of (a) a separation mechanism of a gas mixture through a packed column and (b) sensing mechanism of ZnO QDs when exposed to 2-CEES.

The peak height (Δ Sensor signal) obtained from the mini-GC system is defined as the logarithmic difference in the sensor resistances in air and under target gases. It can be expressed as follows [18].

$$\Delta \text{ Sensor signal} = \log(\text{Resistance})_{max} - \log(\text{Resistance})_{min} \quad (2)$$

where $\log(\text{Resistance})_{max}$ denotes the maximum resistance before the sensor is exposed to the target gas, and $\log(\text{Resistance})_{min}$ is the minimum resistance during the exposure.

For a selectivity test of the sensor, the same measurements were conducted under various gases such as NO_2, NO, and CO. To prepare the gas mixtures, we mixed 5 ppm of each gas with 5 ppm of 2-CEES. As a result, we obtained three different types of gas mixtures: 5 ppm of 2-CEES with 5 ppm of NO_2, 5 ppm of 2-CEES with 5 ppm of NO, and 5 ppm of 2-CEES with 5 ppm of CO.

3. Result and discussion

Fig. 2 shows the mechanisms for the gas separation of a mixed gas passing through the column and the sensing of the ZnO-based sensor. Fig. 2(a) shows a separation mechanism of the mixed gas via the packed column inside the GC device. The mixed gas is passed through the column packed with supporters coated by a stationary phase. We chose a packed column instead of a capillary one, because it is cheap and has high surface area and operability at room temperature [20]. The constant flow of air, which is used as the carrier gas, lets the target gas progress into the column. Thus, the separation of the mixed gases is based on the different strengths of interaction between the gas molecules and the stationary phase. As the filler is a weakly polar material, non-polar gases, such as N_2 and CO_2, proceed faster inside the column than polar gases, such as 2-CEES, because of their similar nature. In addition to the intermolecular interaction, the size of the gas molecules is another factor affecting the gas separation, because gas molecules need to move between the packed materials, and smaller particles can easily penetrate through empty spaces. Therefore, non-polar gases and gases (with smaller gas molecules) are released more rapidly than others, and this variance in the speed of progression inside the column is reflected in the difference in the retention times.

Fig. 2(b) shows a schematic of the 2-CEES sensing mechanism for undoped ZnO and AZO QDs. In an ambient air condition, the electrons in ZnO are captured by oxygen molecules in the air to produce ionic oxygen species, such as O^-, O^{2-}, and O_2^-, on the surface of the QDs. It was reported that most of these oxygen species exist in the O^- ion form at the operating temperature of 450 °C [21]. As free electrons from the conduction band are consumed near the surface of the QDs to generate these functional groups, a thick electron depletion region is formed on the surface. This region creates a high potential barrier, requiring considerable energy for the electrons to migrate intermolecularly and increasing the resistance of the sensing materials. When the undoped ZnO and AZO QDs are exposed to 2-CEES, the target gas reacts with the oxygen species on the surface. Above a temperature of 300 °C, 2-CEES is first decomposed into two radicals: $ClCH_2CH_2\cdot$ and $\cdot SCH_2CH_3$ [12,13]. The two highly active species adsorb onto Lewis acidic sites, such as the metal ions on the metal oxide surface, owing to the Lewis basic characteristics of chlorine and sulfur moieties. After the adsorption, these chemicals are oxidized by reacting with the oxygen species as follows:

$$2ClCH_2CH_2^{\bullet} + 8O^- \rightarrow 2CO_2 + Cl_2 + 4H_2O + 8e^- \quad (3)$$

$$2CH_3CH_2S^{\bullet} + 13O^- \rightarrow 2SO_2 + 5H_2O + 2CO_2 + 13e^- \quad (4)$$

Because of these reactions, the electrons captured by the oxygen molecules are released and transferred back to the interior part of the sensing materials. The gases resulting from the oxidation (CO_2, Cl_2, SO_2, and H_2O) are released during the process. This phenomenon reduces the size of the electron depleted layers of the metal oxides and lowers the potential barrier for intermolecular transport of the electrons, which consequently decreases the sensor resistance. This change in the resistance enables the metal oxide sensors to detect 2-CEES when the gas molecules are adsorbed onto the surface.

The crystal structures of the as-synthesized NPs and QDs were characterized by XRD. Fig. 3(a) shows the XRD patterns of the as-

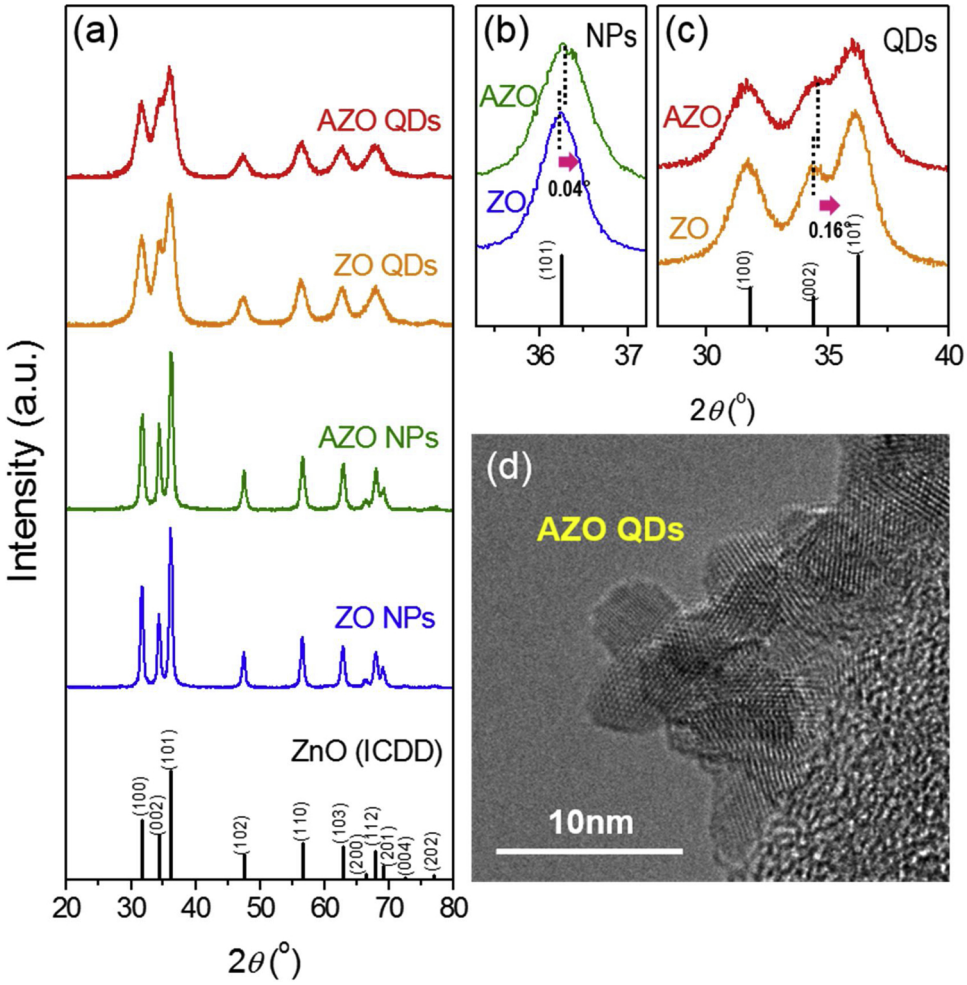

Fig. 3. (a) XRD patterns of ZO and AZO NPs and of ZO and AZO QDs. The vertical lines at the bottom correspond to the standard XRD pattern of hexagonal wurtzite-type ZnO (ICDD: # 98-000-0483), (b) magnified (101) peak for ZO and AZO NPs, (c) magnified peaks of (100), (002), and (101) for ZO and AZO QDs, and (d) high-resolution TEM image of AZO QDs.

synthesized NPs and QDs. The XRD diffraction peaks of the samples were indexed to the crystal structure of the hexagonal wurtzite ZnO phase (ICDD: #98-000-0483), as shown in Fig. 3(a). No other secondary phases or impurity peaks were observed. The peak broadening observed in the XRD patterns of the ZO and AZO QDs clearly indicates that smaller nanocrystals are present in the QD samples. The Al-doped ZnO NPs and QDs show a peak shift to slightly higher angles compared to that of the undoped ZnO NPs and QDs, as shown in Fig. 3(b) and (c), respectively. The shifts were found to be approximately 0.04° for the (101) peak of the AZO NPs and approximately 0.16° for the (002) peak of the AZO QDs. The shift to higher angles is due to the reduction in the interlayer spacing of ZnO along the (101) axis for the AZO NPs and along the (002) axis for the AZO QDs, because Zn^{2+} (with an atomic radius of 0.74 Å) is replaced by Al^{3+}, which has a smaller atomic radius of 0.53 Å. The shifts in the diffraction peak indicate that the Al dopant is well integrated into the ZnO lattice sites in both AZO NPs and AZO QDs. In addition, the shape and size of the as-synthesized nanoparticles were probed using a high-resolution TEM, revealing that the ZO and AZO QDs are spherical with a diameter of ~5 nm. Fig. 3(d) shows the representative TEM image of the AZO QDs. The morphologies of the ZO and AZO NPs show that they have a spherical shape with a diameter of ~30 nm, which is consistent with our previous report [16,17]. The details of the characterization of the undoped ZO and AZO QDs are elucidated in our other paper [19].

The sensing properties of the NPs and QDs were measured to compare their performances in a tube furnace system. Fig. 4 shows the variation in the responses of the NPs and QDs to 20 ppm of 2-CEES as a function of time measured at 450 °C in the tube furnace system. Here, the temperature of 450 °C was found to be the optimal working temperature for ZO and AZO QDs, resulting in the highest sensing responses

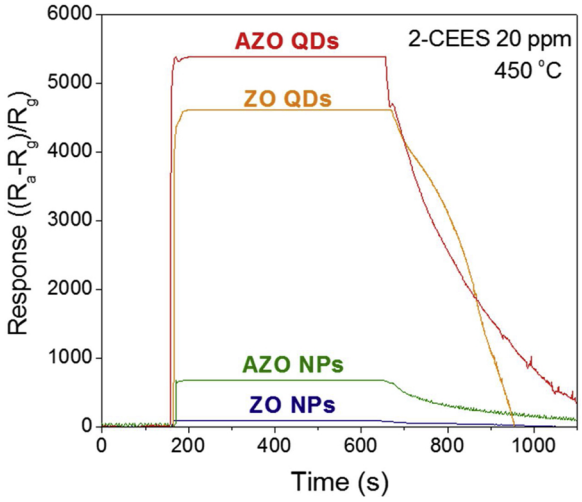

Fig. 4. Sensing responses of ZO NPs, AZO NPs, ZO QDs, and AZO QDs to 20 ppm of 2-CEES at 450 °C measured in a tube furnace system.

Table 1
Comparison of the 2-CEES sensing properties of various types of metal-oxide-based sensors.

Sensing materials	Operating Temperature [°C]	Concentration [ppm]	Response(R_a/R_g)	Sensitivity* [ppm^{-1}]	Response time [s]	Recovery time [s]	Ref.
Al-doped ZnO QDs	450	20	5393	~270	3	406	This work
ZnO QDs	450	20	4614	~231	3	207	This work
Al-doped ZnO NPs	500	20	954	~48	2	127	[17]
ZnO NPs	500	20	344	~17	6	165	[17]
Sm_2O_3 doped SnO_2 NPs	200	10	540	~54	40	20	[14]
SnO_2 NPs	250	10	180	~18	50	20	[14]
Ru-$CdSnO_3$ thin film	350	4	62	~15	5	185	[13]
Pt-$CdSnO_3$ thin film	250	4	59	~15	30	300	[12]
$CdSnO_3$ thin film	350	4	12	~3	2	75	[12]

* sensitivity = response/concentration.

in the tube furnace system. As shown in Fig. 4, the ZO and AZO NPs exhibit sensing responses of ~87 and ~673, respectively, at 450 °C, which are consistent with our previous reports [16,17]. In our previous study [17], the maximum sensing responses of ZO and AZO NPs were found to be approximately 344 and 954, respectively, at an optimal working temperature of 500 °C. The result obtained with AZO NPs [17] was the best sensing response compared to those reported by other groups [12–14] (See Table 1). However, when we conducted the same experiments with ZO and AZO QDs, they exhibited remarkably enhanced responses of 4614 and 5393, respectively, as shown in Fig. 4. According to our knowledge, the result obtained with AZO QDs demonstrates the best sensing performance to 20 ppm of 2-CEES among metal oxide semiconductor sensors, as listed in Table 1. This extraordinary improvement can be attributed to the size effect of the nanoparticles. As the particle size is decreased from 30 nm (NPs) to 5 nm (QDs), the specific surface areas and the number of surface oxygen species increase [19]. These increments are directly related to the increased possibility of chemical reaction between the oxygen species and the radicals. Additionally, as the doping of Al into ZnO is known to increase the response of sensors via the increase in the oxygen vacancies in ZnO lattices [17], the AZO QD sensor a has greater sensing response than the ZO QD sensor. Thus, the AZO QD sensor exhibits the best performance among the fabricated ZnO-based sensors, as shown in Fig. 4.

The AZO QDs showing the best sensing performance in the tube furnace system were investigated as a sensing material for the detection of 2-CEES in the mini-GC system. Fig. 5(a) shows the chromatogram when 1 ml of ambient air, N_2, and 20 ppm of 2-CEES are injected into the mini-GC system equipped with a column (of length 20 cm) and the AZO QD sensor. Only the chromatogram of 2-CEES showed a noticeably large peak at approximately 2000 s at 430 °C, as shown in Fig. 5(a). Here, the temperature of 430 °C was found to be the optimal working temperature for ZO and AZO QDs, showing the highest sensing responses in the mini-GC system. The remaining graphs did not contain any major peaks other than the peaks at 50 s, which correspond to the peak of N_2. Therefore, the results show that the AZO QD sensors were able to detect 20 ppm of 2-CEES in an ambient air environment.

To reduce the retention time of 2-CEES, we optimized the length of the packed column. According to Yang et al., the retention time associated with a gas chromatography system can be described using the following equation [22].

$$\mu = \frac{L}{V_f}[\varepsilon + (1-\varepsilon)RT\rho_c K'] \quad (5)$$

where μ is the retention time, L is the length of the column, V_f is the flow rate of the carrier gas, ε is the porosity, R is the gas constant, ρ_c is the density, and K' is the Henry's constant. According to Eq. (5), the retention time of a gas is directly proportional to the column length. Therefore, to reduce the retention time of 2-CEES, we decreased the column length from 20 cm to 5 cm while maintaining its inner diameter. Fig. 5(b) shows the change in the sensor signal of the AZO QD sensor with respect to the injected gases of air and 20 ppm of 2-CEES at

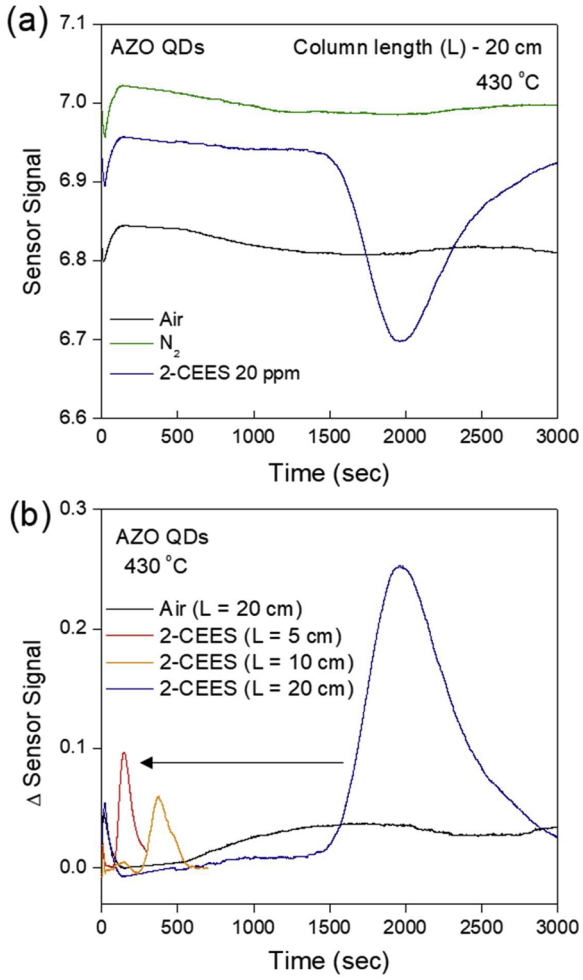

Fig. 5. Sensing performance of the AZO QD sensor tested at an optimized working temperature of 430 °C in the mini-GC device: (a) GC chromatograms for air, N_2, and 20 ppm of 2-CEES, and (b) change in the sensor signal for air and 20 ppm of 2-CEES corresponding to packed column lengths of 5, 10, and 20 cm.

column lengths of 5, 10, and 20 cm. Subsequently, the peak of 2-CEES shifted from 2000s at 20 cm to 375 s at 10 cm and 150 s at 5 cm. Focusing on the fact that the retention time of 150 s for a mustard gas is adequately short, our mini-GC system exhibited excellent detecting ability for the real-time detection of warfare agents.

After optimizing the dimensions of the column, the 2-CEES sensing properties of each sensing material are evaluated under the same condition. Fig. 6(a) shows the variations in the sensor signals of ZO NP, AZO NP, ZO QD, and AZO QD sensors to 20 ppm of 2-CEES for an optimized column length of 5 cm. The height of 2-CEES peak is used to

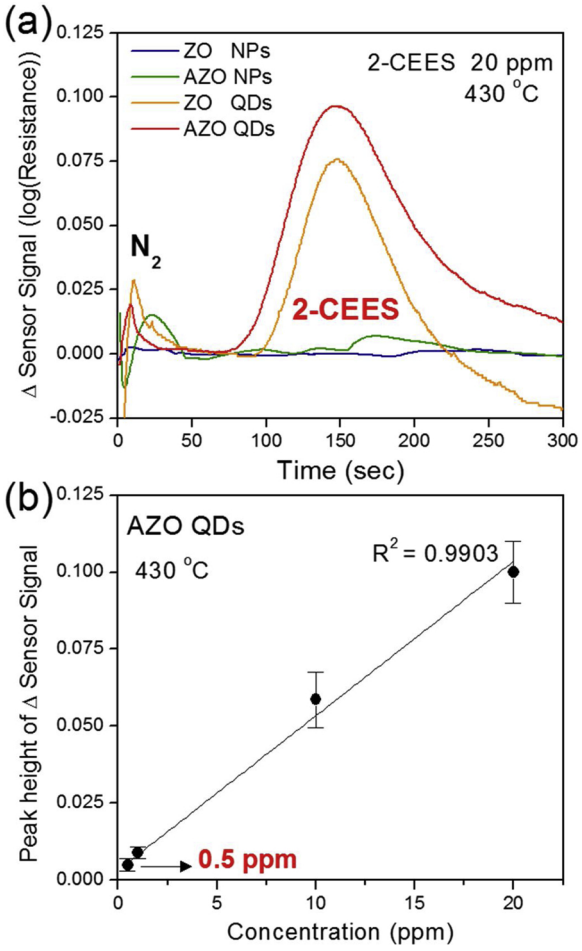

Fig. 6. Sensing performance of the mini-GC device for an optimized column length of 5 cm at 430 °C: (a) Δ Sensor signals of ZO NPs, AZO NPs, ZO QDs, and AZO QDs to 20 ppm of 2-CEES, and (b) peak height of Δ Sensor signal for AZO QDs sensor at various 2-CEES concentrations (0.5–20 ppm) with a calibration curve in the range of 1–20 ppm.

compare their sensing performances. According to Fig. 6(a), the peak height increases with the decrease in the particle size, and the dopants contribute toward further increasing the responses. Although the QDs could be used to detect 2-CEES, the performance of the NPs was poor because of the significantly low sensitivity and the small amount of target gas used. Thus, the AZO QDs exhibited the best performance for the detection of 2-CEES using the mini-GC system.

Fig. 6(b) shows the peak height of the Δ Sensor signal curves obtained from the AZO QD sensor for the N_2-based 2-CEES gas at various concentrations at 430 °C. The peak heights of the AZO QD sensors for 2-CEES concentrations of 0.5, 1, 10, and 20 ppm are estimated to be approximately 0.005, 0.009, 0.0587, and 0.1, respectively. We successfully distinguished the peaks of 0.5 and 1 ppm of 2-CEES, and after considering the signal-to-noise ratio, the detection limit of the AZO QDs sensor was found to be 0.5 ppm. The strong linearity (R^2 = 0.9903) between the 2-CEES concentration and Δ Sensor signal is clearly reflected in the linear fit, as shown in Fig. 6(b). Based on this result, a reliable estimation of the concentration of 2-CEES is possible using our device.

For the in-situ analyzation and detection of 2-CEES, we tested the performance of the mini-GC device with the AZO QD sensor in the selective sensing of a target gas from a mixture of gases. NH_3, NO, and CO (5 ppm each) were mixed with 5 ppm of 2-CEES to prepare three different types of gas mixtures. The gases of NH_3, NO, and CO are selected as interfering gases, because they are often released to air as flue

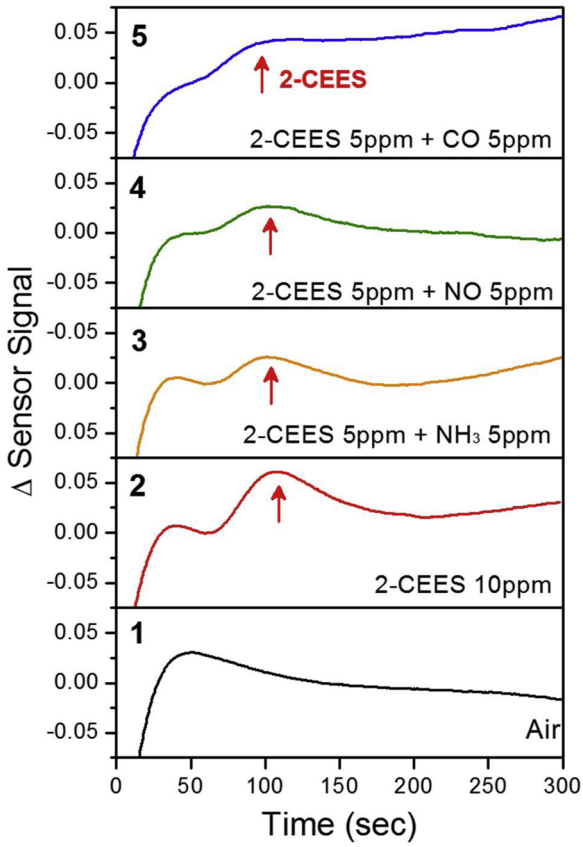

Fig. 7. Selectivity of mini-GC device to air, 10 ppm of 2-CEES, and three different types of gas mixtures (2-CEES 5 ppm and NH_3/NO/CO 5 ppm) tested at 430 °C.

exhaust [22]. As flue gases may exist in any situation involving air pollution or explosion, the sensor must be able to distinguish 2-CEES from them. The chromatograms of the gas mixtures are compared with those of air and 10 ppm of 2-CEES, as shown in Fig. 7. The range of retention times in which 2-CEES can be detected is highlighted with red arrows. As shown in Fig. 7, all the gases except air exhibit the peak of 2-CEES. The peaks of 2-CEES in traces 3˜5 have similar heights compared to each other. In particular, it was observed that the peak height of the traces 3˜5 was about half of that of the trace 2. This is because half of 10 ppm of 2-CEES in trace 2 were injected in traces 3-5. Even with the gas mixtures, no other peaks can be seen from the chromatograms. As reported previously, AZO NPs showed much higher response toward 2-CEES over NH_3, NO, and CO [14]. From this result, we could extrapolate the selective behavior of AZO QDs, which can be explained from the interaction of the gases with the column materials. As the molecular weights of NH_3 (17.031 g/mol), NO (30.01 g/mol), and CO (28.01 g/mol) gases are significantly lower than that of 2-CEES (124.63 g/mol), these gases passed through the packing materials inside the column much faster than 2-CEES, similar to N_2 (28.01 g/mol). As a result, they could be detected at a similar retention time to that of N_2, which is approximately 10 s. Therefore, it was possible to distinguish 2-CEES from the other gases within 150 s via the gas chromatograms obtained using the mini-GC device.

4. Conclusions

In this work, we developed a novel gas chromatography (GC) device with Al-doped ZnO (AZO) QDs and a packed column to selectively detect small amounts of chemical warfare agent simulants, particularly 2-chloroethyl ethyl sulfide (2-CEES). In the tube furnace system, the AZO QDs (d = 5 nm) exhibited a greater sensing response (R = ˜5,393)

toward 2-CEES than AZO NPs (d = 30 nm, R = ~673) at an optimal working temperature of 450 °C. This significant improvement can be attributed to the increased specific surface area obtained by reducing the particle size. It is noteworthy that the sensing response of the AZO QDs to 20 ppm 2-CEES is superior to that of other previously reported 2-CEES sensors based on semiconducting metal oxides.

With the reduction in the length of the packed column in the mini-GC device integrated with AZO QDs from 20 cm to 5 cm, the retention time of 2-CEES was considerably reduced to 150 s from 2000s, making it suitable for real-time detection. However, the AZO NPs could not be used to detect 2-CEES because of the small volume (1 ml) of the target gas and the relatively low sensitivity in ambient condition. The AZO QDs could be used to detect 2-CEES down to 0.5 ppm. More importantly, 5 ppm of 2-CEES was selectively detected using the mini-GC device integrated with the AZO QDs from a mixture of interfering gases such as NH_3, NO, and CO within 150 s. We demonstrated that the mini-GC device integrated with the AZO QDs can be utilized in warfare or counter terrorism applications to quickly detect 2-CEES, as it exhibits high selectivity and sensitivity.

Acknowledgments

This work was supported by the Basic Science Research Program through the National Research Foundation of Korea (NRF), and it was funded by the Ministry of Science, ICT & Future Planning (NRF-2017M3A9F1052297) and the Medium and Large Complex Technology Commercialization Project through the Commercializations Promotion Agency for R&D Outcomes funded by the Ministry of Science and ICT.

References

[1] B. Papirmeister, C.L. Gross, H. Meier, J.P. Petrali, J.B. Johnson, Toxicol. Sci. 5 (1985) 134.
[2] S. Chauhan, S. Chauhan, R. D'Cruz, S. Faruqi, K.K. Singh, S. Varma, M. Singh, V. Karthik, Environ. Toxicol. Pharmacol. 26 (2008) 113–122.
[3] K. Ganesan, S.K. Raza, R. Vijayaaraghavan, J. Pharm. Bioallied Sci. 2 (3) (2010) 166–178.
[4] M.A. Makinen, O.A. Anttalainen, M.E.T. Sillanpaa, Ion mobility spectrometry and its applications in detection of chemical warfare agents, Anal. Chem. 82 (2010) 9594–9600.
[5] R.S. Pilling, G. Bernhardt, C.S. Kim, J. Duncan, C.B. Crothers, D. Kleinschmidt, D.J. Frankel, R.J. Lad, B.G. Frederick, Sens. Actuators B Chem. 96 (2003) 200–214.
[6] F. Petersson, P. Sulzer, C.A. Mayhew, P. Watts, A. Jordan, L. Mark, T.D. Mark, Rapid Commun. Mass Spectrom. 23 (2009) 3875–3880.
[7] N. Taranenko, J. Pierre, D. Stokes, T. Vo-Dinh, J. Raman Spectrosc. 27 (1996) 379–384.
[8] D.E. Tevault, R.E. Pellenbarg, Sci. Total Environ. 73 (1988) 65–69.
[9] G. Sberveglieri, C. Baratto, E. Comini, G. Faglia, M. Ferroni, M. Pardo, A. Ponzoni, A. Vomiero, Thin Solid Films 517 (2009) 6156–6160.
[10] S.C. Lee, H.Y. Choi, S.J. Lee, W.S. Lee, J.S. Huh, D.D. Lee, J.C. Kim, Sens. Actuators B Chem. 137 (2009) 239–245.
[11] S.C. Lee, H.Y. Choi, W.S. Lee, S.J. Lee, D. Ragupathy, D.D. Lee, J.C. Kim, Sens. Lett. 9 (2011) 101–105.
[12] L.A. Patil, V.V. Deo, M.D. Shinde, A.R. Bari, M.P. Kaushik, Sens. Actuators B Chem. 160 (2011) 234–243.
[13] L.A. Patil, V.V. Deo, M.D. Shinde, A.R. Bari, M.P. Kaushik, Sens. Actuators B Chem. 191 (2014) 130–136.
[14] H.M. Aliha, A.A. Khodadadi, Y. Mortazavi, Sens. Actuators B Chem. 181 (2013) 637–643.
[15] N. Barsan, D. Koziej, U. Weimar, Sens. Actuators B Chem. 121 (2007) 18–35.
[16] R. Yoo, C. Oh, M.J. Song, S. Cho, W. Lee, J. Nanosci. Nanotechnol. 18 (2018) 1232–1236.
[17] R. Yoo, D. Lee, S. Cho, W. Lee, Sens. Actuators B Chem. 254 (2018) 1242–1248.
[18] H. Jung, W. Cho, R. Yoo, H.-S. Lee, Y.-S. Choe, J.Y. Jeon, W. Lee, Sens. Actuators B Chem. (2018) online published.
[19] R. Yoo, Y. Park, H. Jung, J.H. Lee, H.-S. Lee, W. Lee, Sens. Actuators B Chem. (2018) to be published.
[20] H.M. McNair, J.M. Miller, Basic Gas Chromatography, John Wiley & Sons Inc, 1997.
[21] C. Wang, L. Yin, L. Zhang, D. Xiang, R. Gao, Sensors 10 (2010) 2088-2016.
[22] K. Tan, S. Zuluaga, Q. Gong, Y. Gao, N. Nijem, J. Li, T. Thonhauser, Y.J. Chabal, Chem. Mater. 27 (2015) 2203–2217.

Jun Ho Lee received a Bachelor's degree and a Master's degree in Material Science and Engineering at Seoul National University in 2015 and 2017, respectively. Since 2017, he is working on development of miniaturized GC integrated with metal oxide based gas sensors as a researcher at Yonsei University.

Hwaebong Jung received a Bachelor's degree in Material Science and Engineering at Yonsei University in 2012. He is currently studying on the breath analyzer using metal oxide based gas sensor as a step toward his Ph.D degree at Yonsei University.

Ran Yoo received her Ph.D. degree in Department of Materials Science and Engineering from Yonsei University in 2018. Her research interests are various nanostructured materials related in chemiresistive gas sensors and breath analyzers. She recently joined Korea Institute of Energy Research in 2018.

Yunji Park received a Bachelor's degree in Chemistry at Kyunghee University in 2017. She recently received her M.S. degree at Yonsei University on the breath analyzer using metal oxide based gas sensor. She joined Samsung Electronics in 2018.

Hyun-sook Lee received her Ph.D. from the Department of Physics of POSTECH in 2008. Now she is a research professor in the Department of Materials Science and Engineering of Yonsei University from 2015. Her research interests are various materials related in high-temperature superconductivity, solid-state hydrogen storage, rare-earth/rare-earth free permanent magnets, nanostructured metal oxide semiconductor gas sensors, and nanostructured thermoelectrics.

Yong-Sahm Choe is a CEO of iSenLab Inc. specialized for R&DB of breath analyzers. He received his B.S, M.S. and Ph. D degrees from the department of metallurgical engineering of Yonsei University in 1989, 1991, 1999, respectively and worked at TYM R&D institute from 1999 to 2011 in Korea. He developed oral malodor diagnosing devices, TWIN BREASOR and TWIN BREASOR II. His research interests are a development of breath analyzers utilizing semiconductor gas sensors and a miniaturization of gas chromatography for breath analyzers.

Wooyoung Lee is the Dean of School of Materials Science and Engineering and the Director of Institute of Nanoscience and Nanotechnology at Yonsei University in Korea. He received a BS degree in Metallurgical Engineering in 1986, a MS degree in Metallurgical Engineering from the Yonsei University in 1988. He received a Ph.D. degree in Physics from University of Cambridge, United Kingdom in 2000. He is a regular member of National Academy of Engineering of Korea. He was a member of National Science & Technology Council and a director in Korea Israel Industrial R&D Foundation. In recent years, his research interests have centered on hydrogen sensors, various metal oxide semiconducting gas sensors, and breath analyzers. He is also studying thermoelectric materials and devices, and permanent magnets. He has received a number of awards in nano-related research areas and a Service Merit Medal (2008) from the Government of Korea due to contribution on the development of intellectual properties. He has authored and co-authored over 200 publications, and has edited three special books on nano-structured materials and devices.